Radboud Universiteit

Selected problems of two-dimensional magnetism

Mikhail Katsnelson

IMM

Institute for Molecules and Materials

Outline

I. Mermin-Wagner, short-range order vs long-range order, and all that
II. False start: K_2CuF_4
III. CrX_3: ferrons, magnetic anisotropy, excitons
IV. CrSBr: highly anisotropic, tunable 2D
V. Fe_3GeTe_2: interplay of phonons and magnetism

Peculiarities of 2D magnets

Soft Goldstone modes in 1D and 2D result in divergent corrections to magnetization which naively means destruction of magnetically ordered state. Rigorous result: the absence of long-range order in 2D Heisenberg model at finite temperatures (Mermin and Wagner, 1966). However, at low temperatures: strong short-range order, exponentially large correlation length (Polyakov, 1975).

Mean-field way to describe the state with short-range order: self-consistent spin wave theory (SSWT), suggested and applied to 2D Heisenberg ferromagnet in different forms by Arovas & Auerbach, 1988; Yoshioka, 1989; Takahashi, 1989.

Easy-axis anisotropy or small interlayer exchange stabilize ordered phase - what to do?

SSWT of 2D magnetism

PHYSICAL REVIEW B VOLUME 60, NUMBER 2 1 JULY 1999-II

Self-consistent spin-wave theory of layered Heisenberg magnets

V. Yu. Irkhin, A. A. Katanin, and M. I. Katsnelson

$$H=-\frac{1}{2}\sum_{ij} J_{ij}\mathbf{S}_i\mathbf{S}_j-\frac{1}{2}\eta\sum_{ij} J_{ij}S_i^zS_j^z-D\sum_i (S_i^z)^2$$

Easy-axis anisotropy

$$\eta>0 \text{ and } D>0$$

Baryakhtar-Krivoruchko-Jablonsky representation **for spin operators**

$$S_i^+=\sqrt{2S}b_i, \quad S_i^z=S-b_i^\dagger b_i-(2S+1)c_i^\dagger c_i,$$

$$S_i^-=\sqrt{2S}\left(b_i^\dagger-\frac{1}{2S}b_i^\dagger b_i^\dagger b_i\right)-\frac{2(2S+1)}{\sqrt{2S}}b_i^\dagger c_i^\dagger c_i, \qquad (2)$$

where $b_i^\dagger, b_i$ are the Bose ideal magnon operators, and $c_i^\dagger, c_i$ are the auxiliary pseudofermion operators at the site i which take into account the kinematic interaction of spin waves.

Treat anharmonic (multimagnon) terms in Hartree-Fock-style way

SSWT of 2D magnetism II

Another useful representation of spin operators is the Schwinger-boson representation

$$\mathbf{S}_i = \sum_{\sigma\sigma'} s^{\dagger}_{i\sigma} \boldsymbol{\sigma}_{\sigma\sigma'} s_{i\sigma'} , \qquad (6)$$

where $\boldsymbol{\sigma}$ are the Pauli matrices, $\sigma, \sigma' = \uparrow, \downarrow$, so that

$$S^z_i = \frac{1}{2}(s^{\dagger}_{i\uparrow} s_{i\uparrow} - s^{\dagger}_{i\downarrow} s_{i\downarrow}), \quad S^+_i = s^{\dagger}_{i\uparrow} s_{i\downarrow} , \quad S^-_i = s^{\dagger}_{i\downarrow} s_{i\uparrow} . \qquad (7)$$

The constraint condition

$$s^{\dagger}_{i\uparrow} s_{i\uparrow} + s^{\dagger}_{i\downarrow} s_{i\downarrow} = 2S \qquad (8)$$

Alternative way: looks nicer but leads to some wrong numerical factors which should be eliminated by hands

SSWT of 2D magnetism III

Apart from magnetization – short-range order parameter describing magnon coupling on neighboring sites

$$\gamma = \overline{S} + \langle b_i^\dagger b_{i+\delta_\perp} \rangle, \qquad \gamma' = \overline{S} + \langle b_i^\dagger b_{i+\delta_\parallel} \rangle$$

Layered 2D FM, no anisotropy, square-lattice in plane

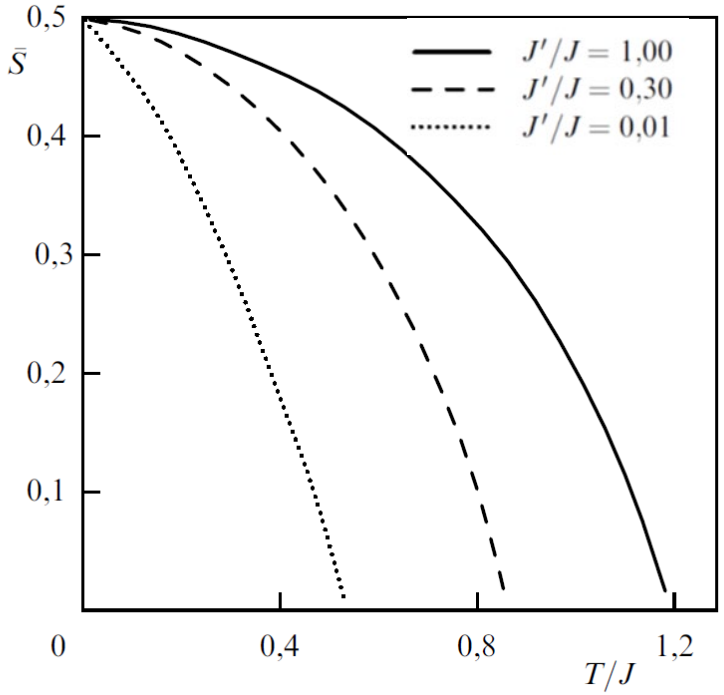

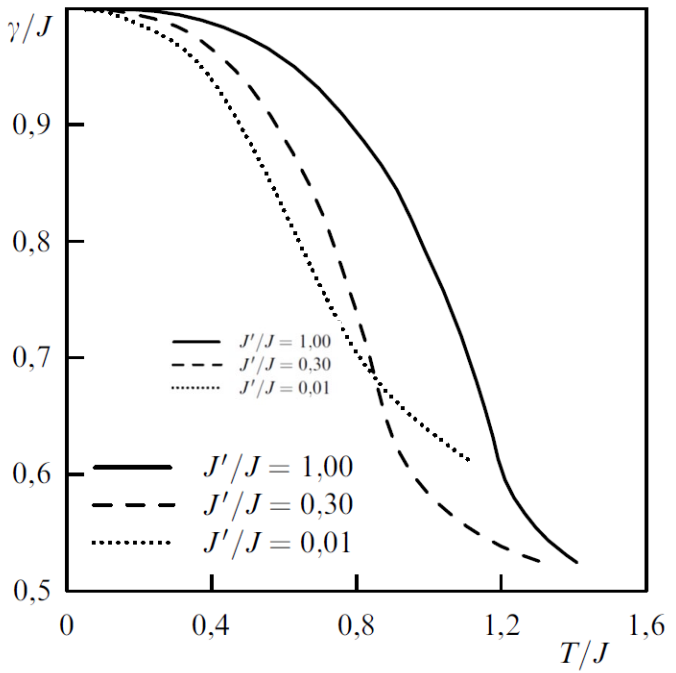

SSWT of 2D magnetism IV

Logarithmic suppression of critical temperature; calculations beyond mean-field (ladder diagrams) are important

TABLE I. The experimental parameters and ordering temperatures of layered magnets and the corresponding calculated values of T_M in the standard spin-wave-theory (SWT), SSWT, and RPA (in brackets taking into account the constant $C_{AF}=-0.7$).

Compound	S	J (K)	J' (K)	Δ_0	T_M^{SWT} (K)	T_M^{SSWT} (K)	T_M^{RPA} (K)	T_M^{exp} (K)
La_2CuO_4	1/2	1600	0.8	≈ 0	672	537	343	325
K_2NiF_4	1	102	≈ 0	0.0088	160	125	90.0 (97.0)	97.1
Rb_2NiF_4	1	82	≈ 0	0.046	180	118	88.4 (95.0)	94.5
K_2MnF_4	5/2	8.4	≈ 0	0.015	74.8	52.1	42.7 (45.1)	42.1
$CrBr_3$	3/2	12.38	1.0	0.024	79.2	51.2	39.0	40.0

In the case of easy-plane anisotropy – no true long-range order, BKT transtion. But…

Dipole-dipole interactions in 2D magnetism

$$\mathcal{H}_{\rm dip} = (g_e \mu_{\rm B})^2 \sum_{i<j} \left[\frac{(|\vec{r}_{ij}|^2 (\hat{\vec{S}}_i \cdot \hat{\vec{S}}_j) - 3(\hat{\vec{S}}_i \cdot \vec{r}_{ij})(\hat{\vec{S}}_j \cdot \vec{r}_{ij})}{|\vec{r}_{ij}|^5} \right]$$

Long-range interaction formally violating conditions of Mermin-Wagner theorem. Tradition: to identify it with easy-plane shape-anisotropy. But: they are equivalent only for homogeneous magnetization and elliptic samples, statistical mechanics is totally different!

Maleev (1976): should be true long-range order since spin-wave spectrum is much harder: $\epsilon_k \sim k^{1/2}$

Confirmed by SSWT – will be important for discussions of $CrCl_3$

PHYSICAL REVIEW B **71**, 024427 (2005)

Thermodynamics of a two-dimensional Heisenberg ferromagnet with dipolar interaction

Alexei Grechnev,[1,*] Valentin Yu. Irkhin,[1,2] Mikhail I. Katsnelson,[1,3] and Olle Eriksson[1]

True long-range order at small T, first-order transition (?!)

The first attempt: K_2CuF_4

RAPID COMMUNICATIONS

PHYSICAL REVIEW B **88**, 201402(R) (2013)

Ferromagnetic two-dimensional crystals: Single layers of K_2CuF_4

B. Sachs,[1,*] T. O. Wehling,[2,3] K. S. Novoselov,[4] A. I. Lichtenstein,[1] and M. I. Katsnelson[5]

FM in layers, very weak AFM coupling between layers, very 2D – why not?

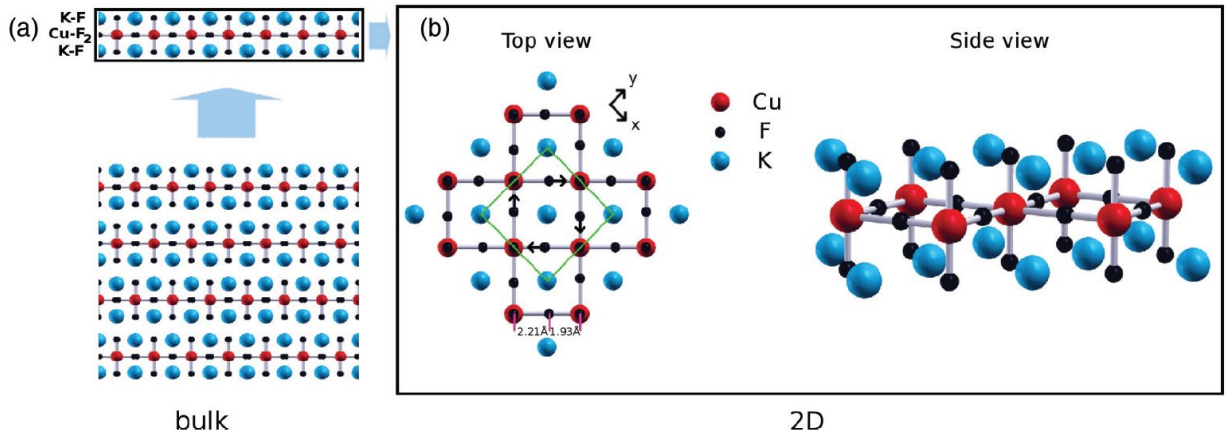

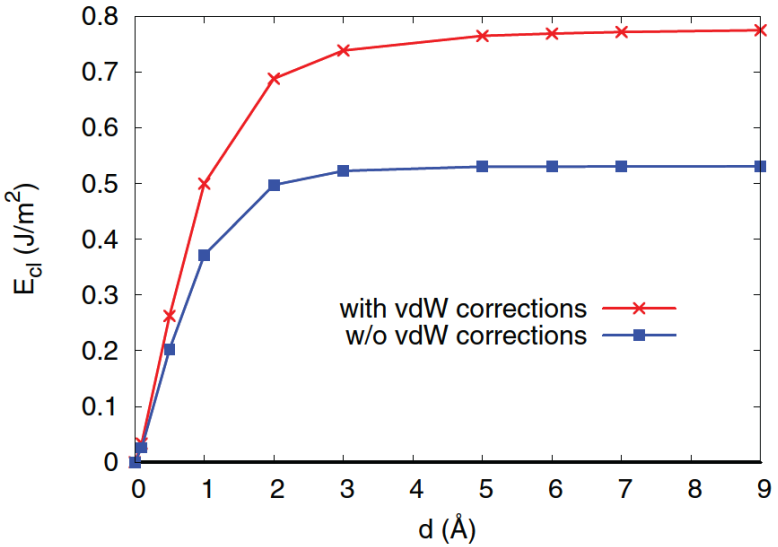

Cohesive energy is just 2-3 times larger than in graphite – exfoliation should be possible?!

The first attempt: K_2CuF_4 II

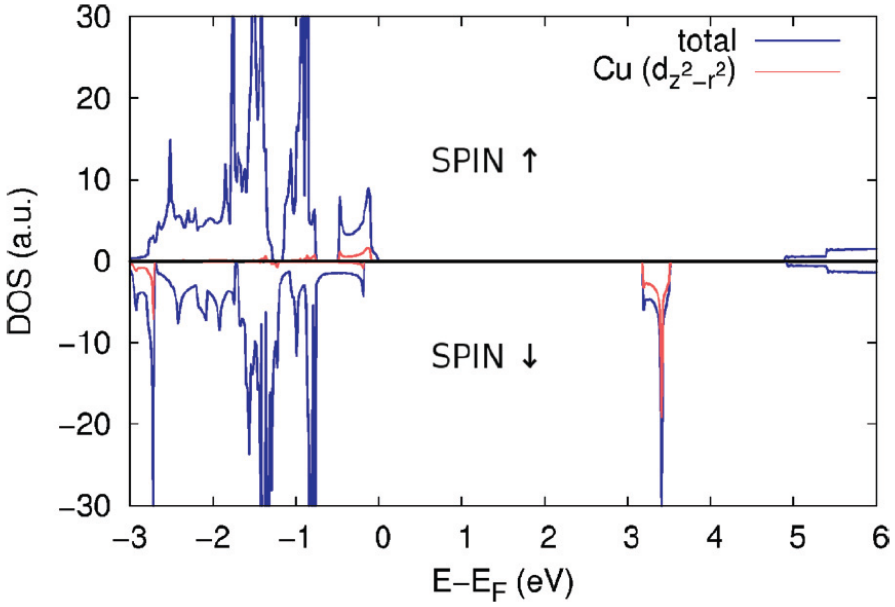

$$H = -\frac{1}{2}\sum_{\langle i,j\rangle} J\left[S_i^x S_j^x + S_i^y S_j^y + \eta S_i^z S_j^z\right]$$

LDA+U results for single layer

$$J/k_B = 25.3 \text{ K and } \eta = 0.90$$

Theoretical estimate of Kosterlitz-Thouless temperature about 8K.

May be still worth to try?! Small spin, strong quantum effects, BKT physics… Yes, temperatures are small but not too small

CrX_3: electronic structure

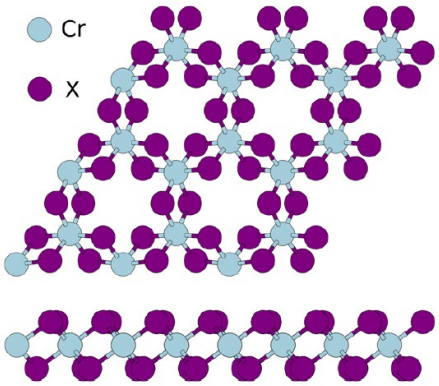

X=Cl, Br, I; probably, the most polular 2D magnets now, with reasonably high Curie temperatures

Correlation effects beyond DFT are important, DFT+U is not sufficient

PHYSICAL REVIEW B **105**, 205124 (2022)

DMFT:

Dynamical correlations in single-layer CrI_3

Yaroslav O. Kvashnin,[1] Alexander N. Rudenko,[2,*] Patrik Thunström,[1] Malte Rösner,[2] and Mikhail I. Katsnelson[2]

PHYSICAL REVIEW B **104**, 155109 (2021)

GW+BSE:

Electronic structure of chromium trihalides beyond density functional theory

Swagata Acharya,[1,*] Dimitar Pashov,[2] Brian Cunningham,[3] Alexander N. Rudenko,[1] Malte Rösner,[1] Myrta Grüning,[4] Mark van Schilfgaarde,[2,5] and Mikhail I. Katsnelson[1]

Importance of charge self-consistency in first-principles description of strongly correlated systems

Swagata Acharya[1]✉, Dimitar Pashov[2], Alexander N. Rudenko[1], Malte Rösner[1], Mark van Schilfgaarde[2,3] and Mikhail I. Katsnelson[1]

npj Computational Materials (2021)7:208

CrX_3: electronic structure II

Here we will focus on QSGW (+ BSE) results. The key effect is the contribution of Cr 3d states and ligand p-states into the valence band – different methods give different results; and of course the gap value!

Spectral weight of halogens in window (- 6 eV, 0 eV); ML – monolayer

	ML band gap (eV)			ML spectral weight			Bulk band gap (eV)		
Theory	$CrCl_3$	$CrBr_3$	CrI_3	$CrCl_3$	$CrBr_3$	CrI_3	$CrCl_3$	$CrBr_3$	CrI_3
LDA	1.51	1.30	1.06	21%	26%	42%	1.38	1.2	0.91
QSGW	6.87	5.73	3.25	40%	63%	81%	5.4	4.38	3.0
QS$G\widehat{W}$	5.55	4.65	2.9	24%	31%	64%	4.4	3.5	2.5

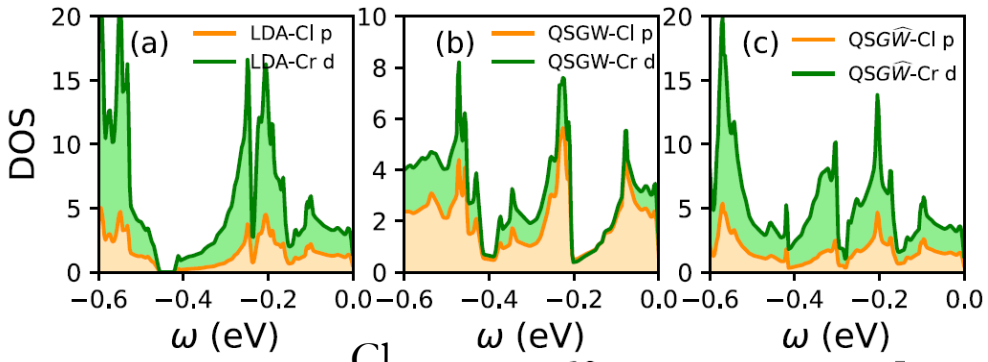

Cl

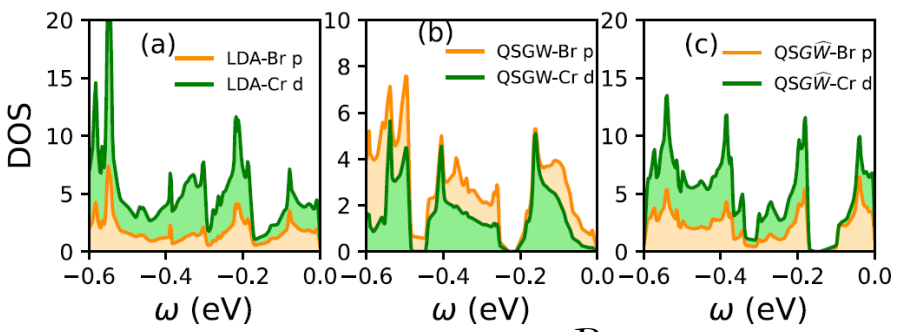

Br

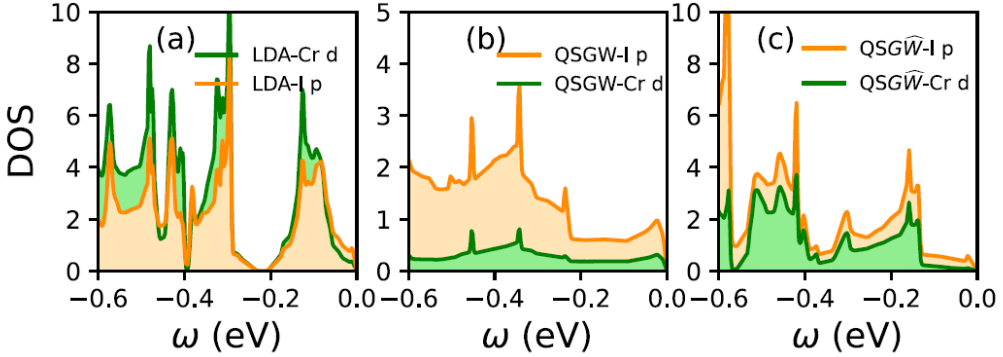

I

CrX_3: optics and excitons

Real- and momentum-space description of the excitons in bulk and monolayer chromium tri-halides

npj 2D Materials and Applications (2022)6:33

Swagata Acharya[1]✉, Dimitar Pashov[2], Alexander N. Rudenko[1], Malte Rösner[1], Mark van Schilfgaarde[2,3] and Mikhail I. Katsnelson[1]

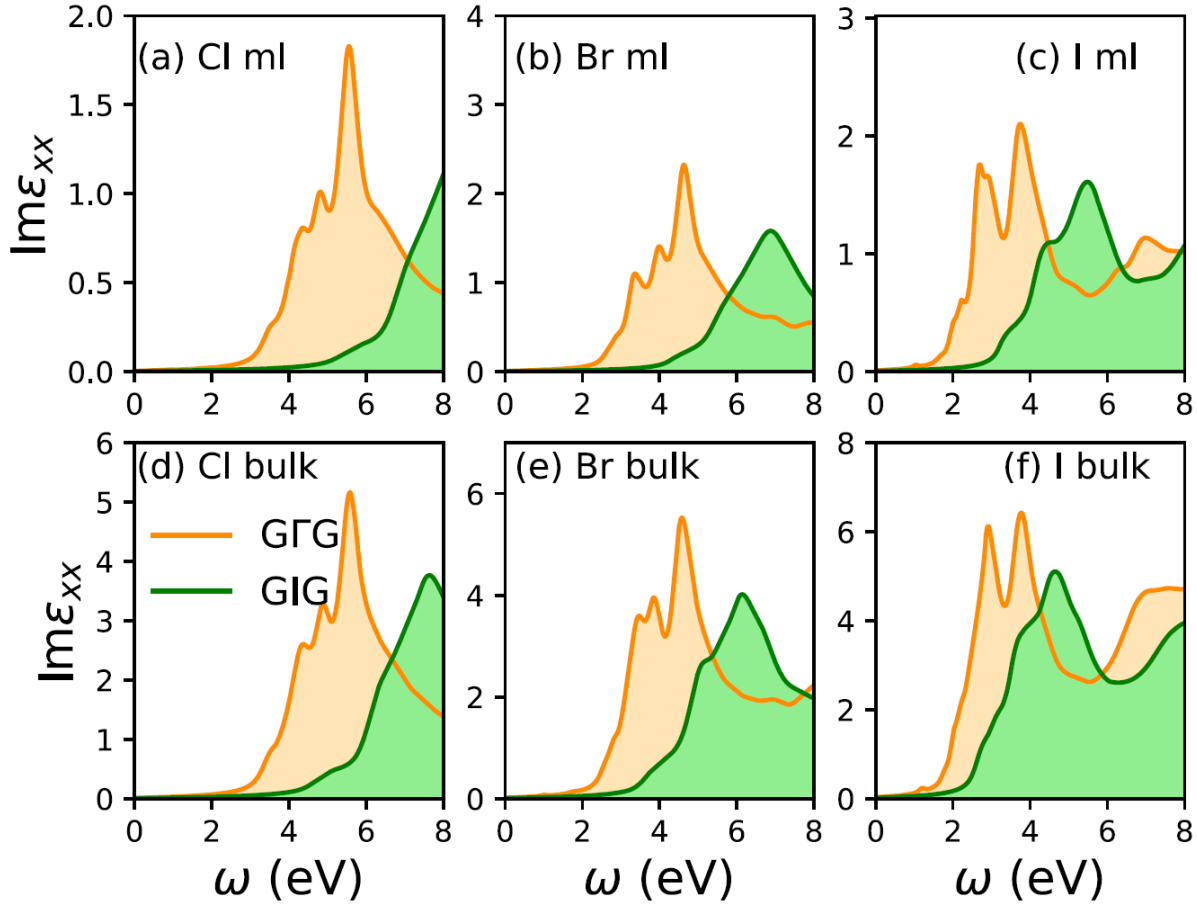

Orange – with vertex (that is, with excitons), green – just G*G

CrX_3: optics and excitons II

When we increase d-p hybridization in the consequence Cl-Br-I, the deepest excitons become more delocalized but they are always close to Frenkel (local), limit than to Wannier-Mott limit

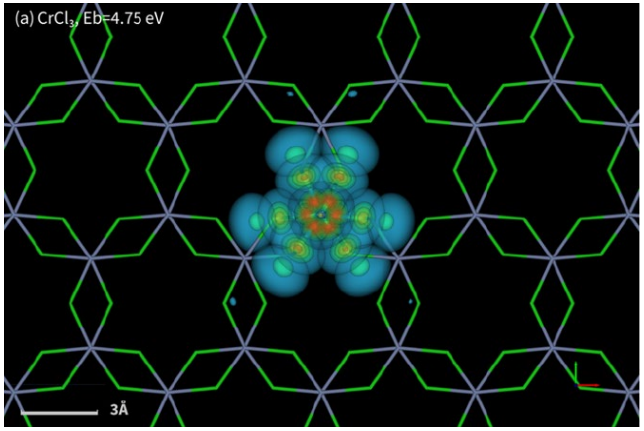

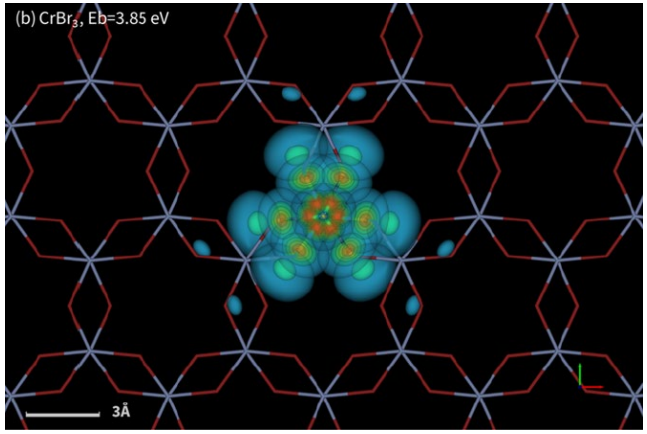

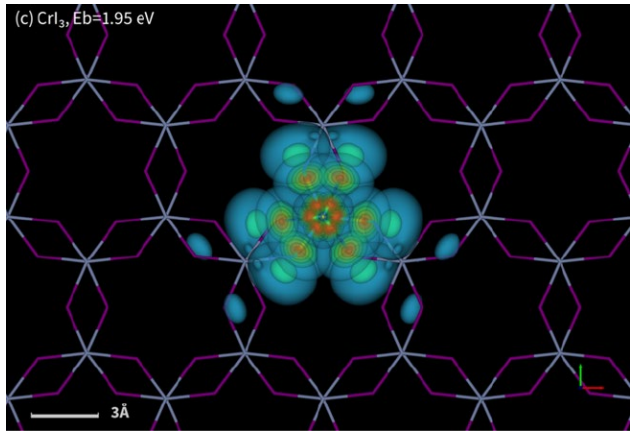

To compare: true Wannier-Mott excitons in MoS_2

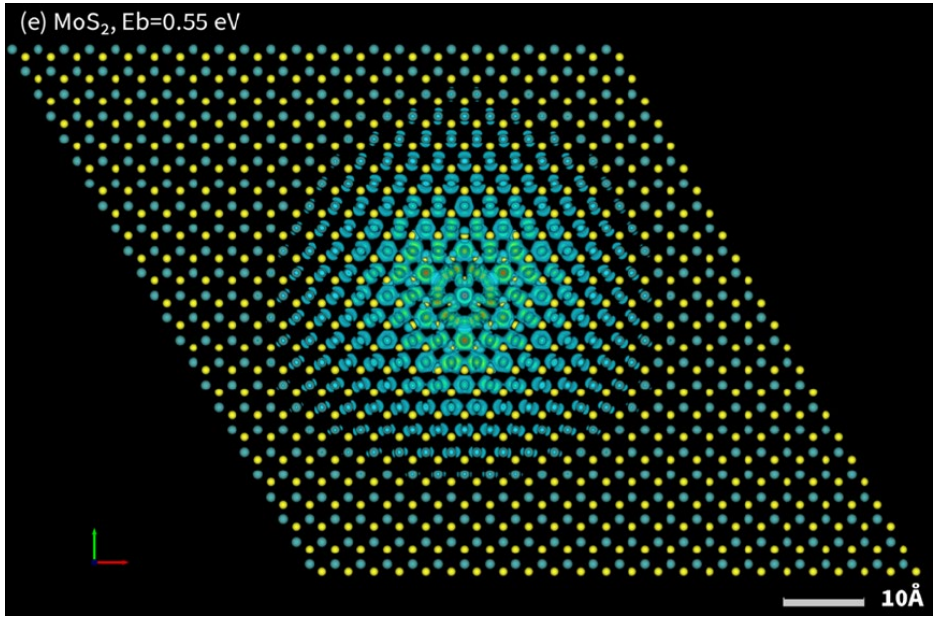

CrX_3: optics and excitons: Experiment

Strongly Correlated Exciton-Magnetization System for Optical Spin Pumping in $CrBr_3$ and CrI_3.

Adv. Mater. **2023**, *35*, 2209513

*M. Grzeszczyk, S. Acharya, D. Pashov, Z. Chen, K. Vaklinova, M. van Schilfgaarde, K. Watanabe, T. Taniguchi, K. S. Novoselov, M. I. Katsnelson, and M. Koperski**

Luminescence in magnetic field shows opposite signs of effective e-h exchange coupling in excitons in $CrBr_3$ and CrI_3

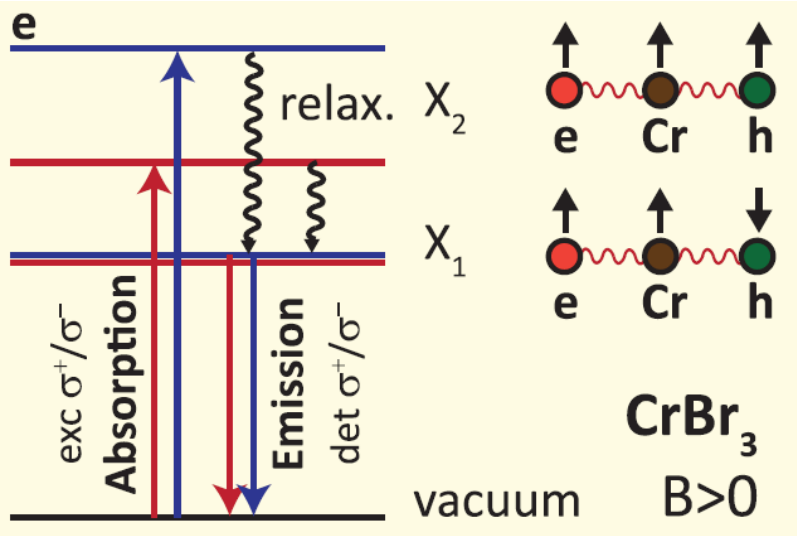

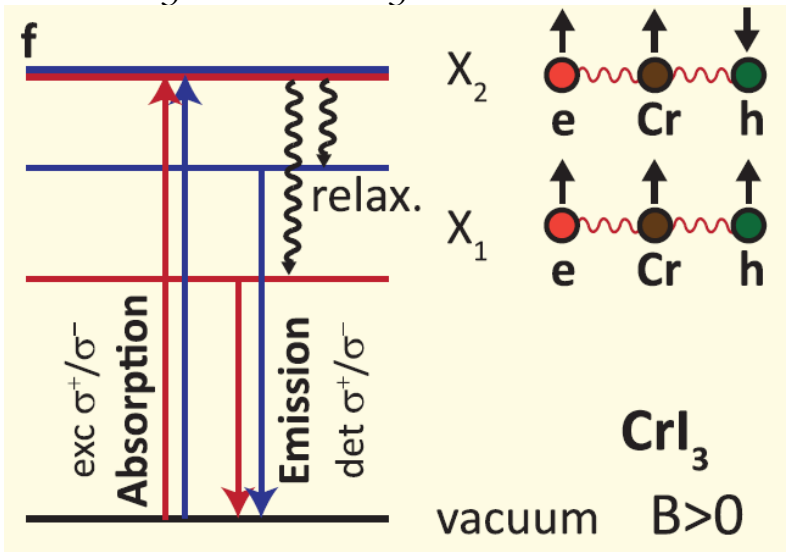

	Ground excitonic state		Excited excitonic state	
	Cr-electron	Cr-hole	Cr-electron	Cr-hole
$CrBr_3$	FM	AFM	FM	FM
CrI_3	FM	FM (small exchange constant)	FM	AFM

CrX_3: optics and excitons: Interpretation

Different role of d-d exchange with Cr atom (always FM, Hund exchange) and d-p exchange between Cr and halogen (always AFM, via Schrieffer-Wolf transformation). Small differences in the composition:

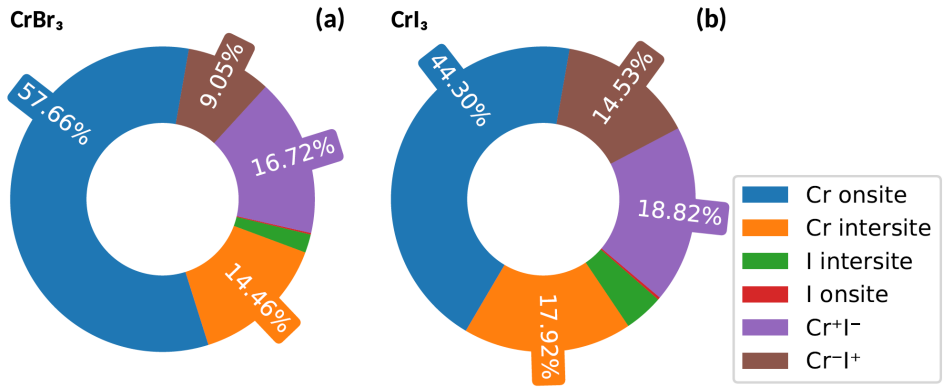

FIGURE S14 Frenkel and charge transfer components for first excited exciton (ex1) state in $CrBr_3$ (a) at 2.0 eV and in CrI_3 (b) at 1.9 eV.

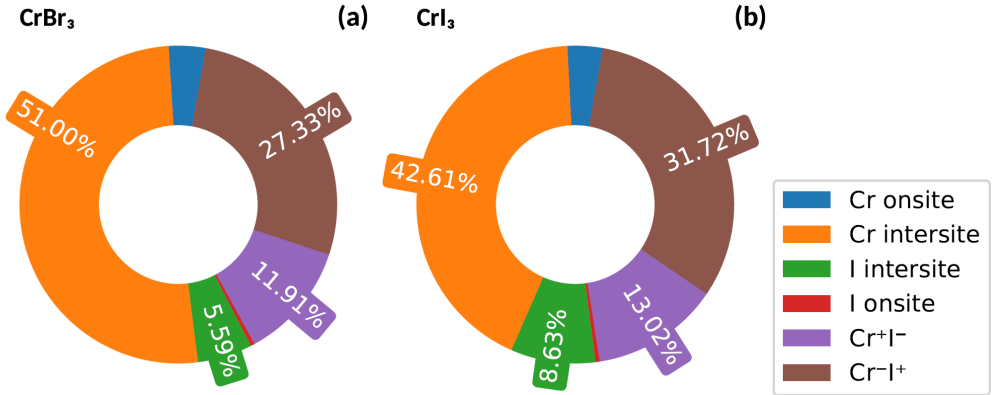

FIGURE S17 Frenkel and charge transfer components for second excited exciton (ex2) state in $CrBr_3$ (a) at 2.8 eV and in CrI_3 (b) at 2.2 eV.

Qualitatively: effective d-p exchange is FM when look at the whole valence band and AFM when look at its top; contributions of different energy regions are also different

Magnetic interactions in CrX_3

Correlation effects are important: quantum chemistry instead of DFT-based

Electronic excitations and spin interactions in chromium trihalides from embedded many-body wavefunctions

npj 2D Materials and Applications | (2024)8:56

Ravi Yadav[1,2], Lei Xu[3,7], Michele Pizzochero[4], Jeroen van den Brink[3,5], Mikhail I. Katsnelson[6] & Oleg V. Yazyev[1,2]

Embedding models used in calcualtions of intra-site and inter-site magnetic interactions

$$\mathcal{H} = \mathcal{H}^1 + \mathcal{H}^2$$

$$\mathcal{H}^1 = \sum_i \vec{S}_i \cdot \bar{\bar{D}}_{\text{sia}} \cdot \vec{S}_i + \sum_i \mu_B \vec{B} \cdot \bar{\bar{g}} \cdot \vec{S}_i$$

$$\mathcal{H}^2 = J_1 \sum_{i<j} (\vec{S}_i \cdot \vec{S}_j) + J_2 \sum_{i<j} (\vec{S}_i \cdot \vec{S}_j)^2 + \sum_{i<j} \vec{S}_i \cdot \bar{\bar{\Gamma}} \cdot \vec{S}_j$$

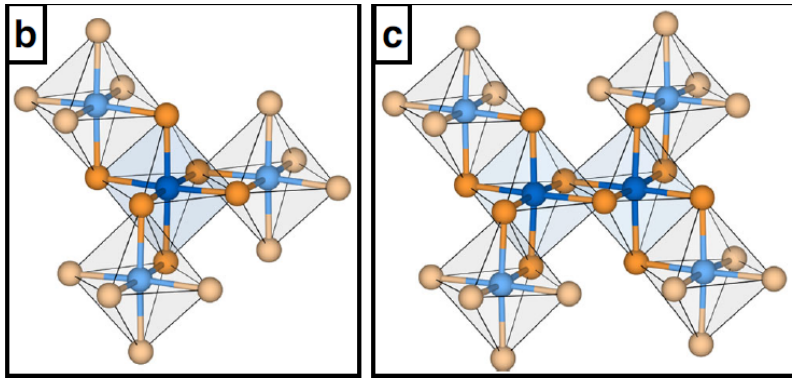

$$\bar{\bar{\Gamma}} = \begin{pmatrix} 0 & \Gamma_{xy} & -\Gamma_{yz} \\ \Gamma_{xy} & 0 & \Gamma_{yz} \\ -\Gamma_{yz} & \Gamma_{yz} & K \end{pmatrix}$$

K is the Kitaev interaction parameter

Magnetic interactions in CrX_3 II

Table 4 | Inter-site magnetic interactions in CrX_3 (X = Cl, Br, I), i.e., bilinear (J_1) and biquadratic (J_2) exchange couplings, along with the off-diagonal (Γ_{xy}, Γ_{yz}, Γ_{zx}) and Kitaev (K) parameters comprised in the symmetric anisotropic tensors, as obtained from the CASSCF and MRCI calculations

	$CrCl_3$		$CrBr_3$		CrI_3	
	CASSCF	MRCI	CASSCF	MRCI	CASSCF	MRCI
J_1 (meV)	−0.64	−0.97	−0.61	−1.21	−0.60	−1.38
J_2 (meV)	−0.04	−0.05	−0.05	−0.05	−0.06	−0.06
Γ_{xy} (meV)	-1.2×10^{-4}	-2.1×10^{-4}	-6.9×10^{-4}	-0.8×10^{-3}	-1.2×10^{-3}	-4.2×10^{-4}
$\Gamma_{yz} = -\Gamma_{zx}$ (meV)	-1.3×10^{-5}	-0.8×10^{-4}	-6.9×10^{-4}	-0.9×10^{-3}	-1.1×10^{-4}	-3.1×10^{-4}
K (meV)	-1.7×10^{-4}	-1.1×10^{-4}	-8.2×10^{-3}	−0.01	-9.3×10^{-3}	−0.05

Biquadratic exchange is weak, Kitaev interaction is extremely weak

Table 3 | Comparison of the dipolar anisotropy parameter A_{dip} and the single-ion anisotropy parameter A_{sia} obtained from MRCI calculations for bulk CrX_3 (X = Cl, Br, I)

	$CrCl_3$	$CrBr_3$	CrI_3
A_{sia} (μeV)	−31.4	−81.1	−124.2
A_{dip} (μeV)	85.2	75.5	57.3

The negative sign indicates that the out-of-plane spin moments are favored. The shape anisotropy parameter A_{dip} for monolayer CrX_3 (X = Cl, Br, I) approximately doubles in magnitude as compared to the bulk, and attains values of 144 μeV, 121 μeV, 94 μeV for chloride, bromide and iodide, respectively.

For X = I, magnetocrystalline anisotropy wins for sure, easy-axis magnetism. For X = Cl, dipole-dipole wins, in-plane magnetization but true long-range order rather than BKT. For X = Br, they are comparable.

Magnetic polaron in bilayer CrI_3

General statement: small doping of magnetic insulators always favor FM since it is more favorable for one electron (or hole) move in FM environment (Zener double exchange, Nagaoka ferromagnetism…)

Idea: if concentration of electrons is not sufficient to establish FM order in the whole crystal, it can be established locally: charge carriers are self-trapped in FM droplet

Ferron (Nagaev), fluctuon (Krivoglaz), magnetic polaron (Mott and many others)…

Formal theory based on path integral formalism: Auslender & MIK 1980-1982

Example: effective spin Hamiltonian for narrow-band Hubbard (or s-d exchange) model at Bethe lattice (Auslender & MIK 1982)

$$\Phi(\{n_i\}) \approx \text{const} + \frac{zt^2}{2\varepsilon_0}\sum_i \cos\theta_i - \left(\frac{8}{15\pi z^{1/2}}\right) z|t| \sum_i \cos\left(\frac{\theta_i}{2}\right)\left(\frac{\tilde{\mu}-E_{11}}{z^{1/2}|t|\cos(\theta_i/2)}\right)^{5/2}\Theta(\tilde{\mu}-E_{11}); \quad \Theta(x)=\begin{cases}1, & x>0,\\ 0, & x<0.\end{cases}$$

$$\cos\theta_i = z^{-1}\sum_\delta (n_i n_{i+\delta})$$

Favors phase separation!

Magnetic polaron in bilayer CrI_3 II

PHYSICAL REVIEW B **101**, 041402(R) (2020)

Rapid Communications | Editors' Suggestion

Magnetic polaron and antiferromagnetic-ferromagnetic transition in doped bilayer CrI_3

D. Soriano and M. I. Katsnelson

Application to AFM bilayer CrI3 (contrary to bulk, interlayer exchange is AFM)

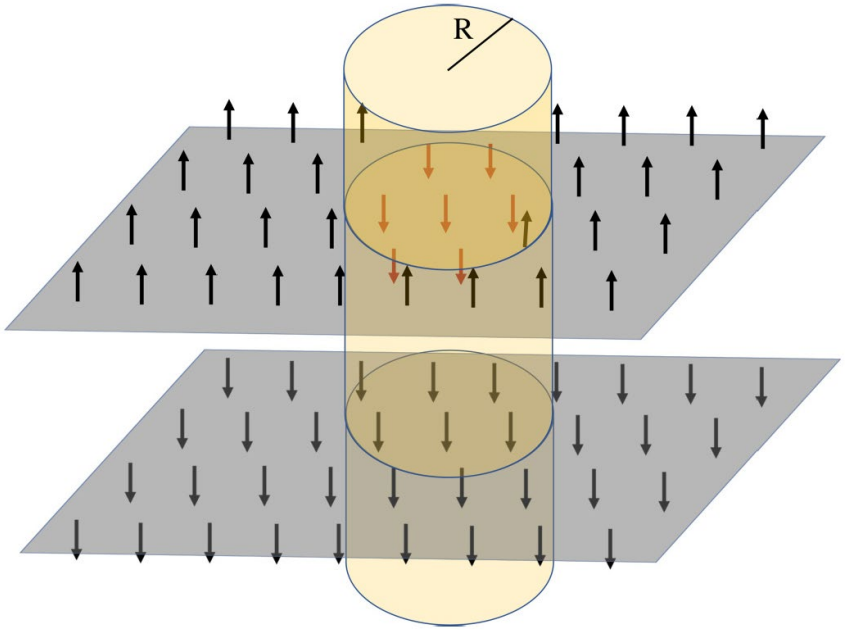

Simple estimate due to Mott (1974)

$$\mathcal{E}(R) = -\Delta + \frac{\hbar^2 z_0^2}{2m^* R^2} + J\frac{\pi R^2}{S_0}, \qquad (2)$$

where the first term Δ is the carrier energy difference between parallel and antiparallel interlayer magnetization, namely, $\Delta_{e(h)} = |\epsilon^{\mathrm{AFM}}_{\mathrm{CB(VB)}} - \epsilon^{\mathrm{FM}}_{\mathrm{CB(VB)}}|$, where VB and CB stand for the top and bottom of valence and conduction bands, respectively. The second term is the energy of a particle confined in a disk of radius R (Fig. 1), with $z_0 = 2.404\,83$ being the first zero of the Bessel function $J_0(z)$, and m^* is the corresponding effective carrier mass in the ferromagnetic state. The third term is the exchange energy needed to switch the magnetic interaction between adjacent layers, where J is the interlayer exchange coupling per magnetic atom, $S_0 = 3a^2\sqrt{3}/4$ is the area occupied by a single Cr atom in the unit cell, and a is the Cr-Cr intralayer distance.

Optimal energy and radius:

$$W = \frac{\hbar^2}{2m^* a^2} \qquad \frac{R^*}{a} = \left(\frac{W}{J}\frac{z_0^2 3\sqrt{3}}{4\pi}\right)^{1/4} \qquad \mathcal{E} = -\Delta + 2\sqrt{WJ\frac{4\pi z_0^2}{3\sqrt{3}}}$$

Magnetic polaron in bilayer CrI_3 III

Simple DFT estimate:

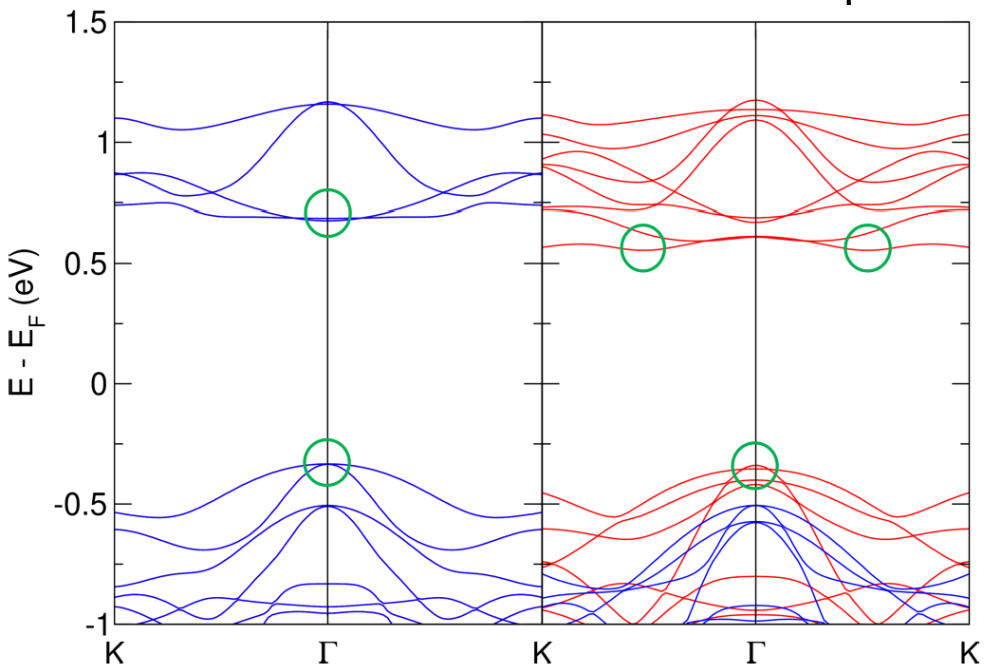

FIG. 3. Band structure of monoclinic bilayer CrI_3 for AFM (left) and FM (right) interlayer exchange. The green circles denote the maximum and minimum of the valence and conduction bands, respectively.

TABLE I. Summary of the parameters obtained from first principles (m_e is the free electron mass).

	VBMax (eV)	CBMin (eV)	m_h^*/m_e	m_e^*/m_e
AFM	−0.333	0.678	0.15	0.18
FM	−0.339	0.555	0.02	0.11

$$\Delta_e \approx 123 \text{ meV and } \Delta_h \approx 6 \text{ meV}$$

$$(R_e^*/a) = 28.4 \text{ and } (R_h^*/a) = 43.4$$

$$\mathcal{E}_e = -91.3 \text{ meV and } \mathcal{E}_h = 67.9 \text{ meV}$$

Prediction: for hole-doped case self-trapping is impossible but for electron-doped case it is, With self-localization energy about 100 meV

CrSBr: tunability of magnetic properties

Dielectric tunability of magnetic properties in orthorhombic ferromagnetic monolayer CrSBr

Alexander N. Rudenko[1] ✉, Malte Rösner[1] and Mikhail I. Katsnelson[1]

npj Computational Materials (2023)9:83

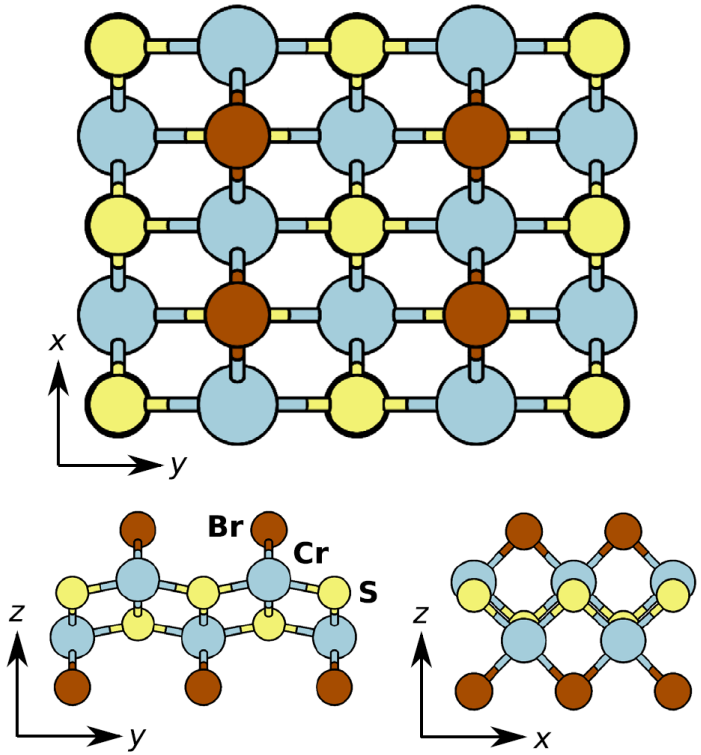

Fig. 1 Schematic crystal structure of monolayer CrSBr shown in three different projections. Brown, blue, and yellow balls correspond to Br, Cr, and S atoms, respectively.

Highly anisotropic crystal structure, FM in monolayer with Curie temperature 146 K

Correlations are very important, minimal method is DFT+U but U should be calculated ab initio

Table 1. WFCE + cRPA averaged local Cr *d* Coulomb matrix elements as a function of the screening from a dielectric encapsulation of the CrSBr monolayer.

ε_{env}	U (eV)	U' (eV)	J_H (eV)	$U_{\text{eff}} = U - J_H$ (eV)
1	3.68	2.86	0.39	3.28
2	3.15	2.34	0.39	2.76
4	2.74	1.93	0.39	2.35
8	2.43	1.61	0.39	2.03
16	2.20	1.39	0.39	1.81
32	2.06	1.25	0.39	1.67
64	1.98	1.17	0.39	1.58
∞[a]	1.90	1.08	0.39	1.40

CrSBr: tunability of magnetic properties II

Magnetic Hamiltonian (parameters from fitting to DFT+U total energies of differet spin connfigularions)

$$H = H_0 + H_{\mathrm{SIA}} + H_{\mathrm{AE}} + H_{\mathrm{D}}$$

$$H_0 = \sum_{ij} J_{ij} \mathbf{S}_i \mathbf{S}_j \qquad H_{\mathrm{SIA}} = D \sum_i \left(S_i^y\right)^2 + E \sum_i \left[\left(S_i^z\right)^2 - \left(S_i^x\right)^2\right]$$

$$H_{\mathrm{AE}} = \sum_{ij} K_{ij} S_i^y S_j^y + \sum_{ij} \Gamma_{ij} \left(S_i^z S_j^z - S_i^x S_j^x\right)$$

$$H_{\mathrm{D}} = \frac{\Omega}{2} \sum_{ij} \frac{1}{|\mathbf{R}_{ij}|^3} \left(\mathbf{S}_i \mathbf{S}_j - 3 \frac{(\mathbf{S}_i \cdot \mathbf{R}_{ij})(\mathbf{S}_j \cdot \mathbf{R}_{ij})}{\mathbf{R}_{ij}^2}\right)$$

CrSBr: tunability of magnetic properties III

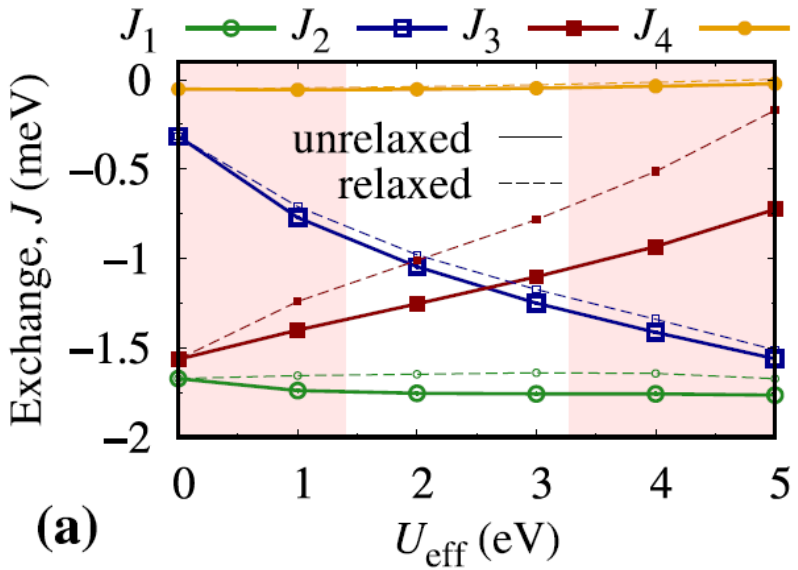

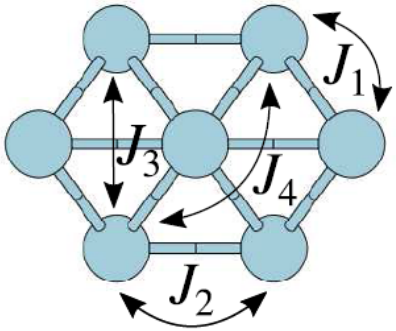

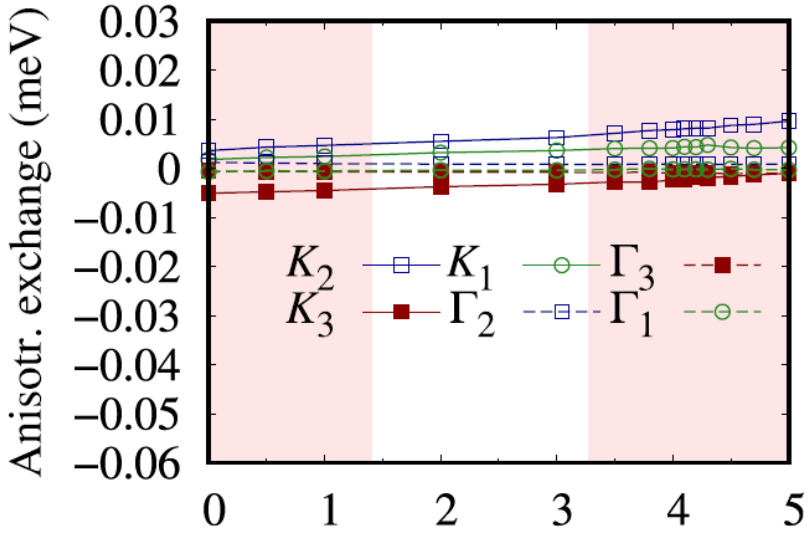

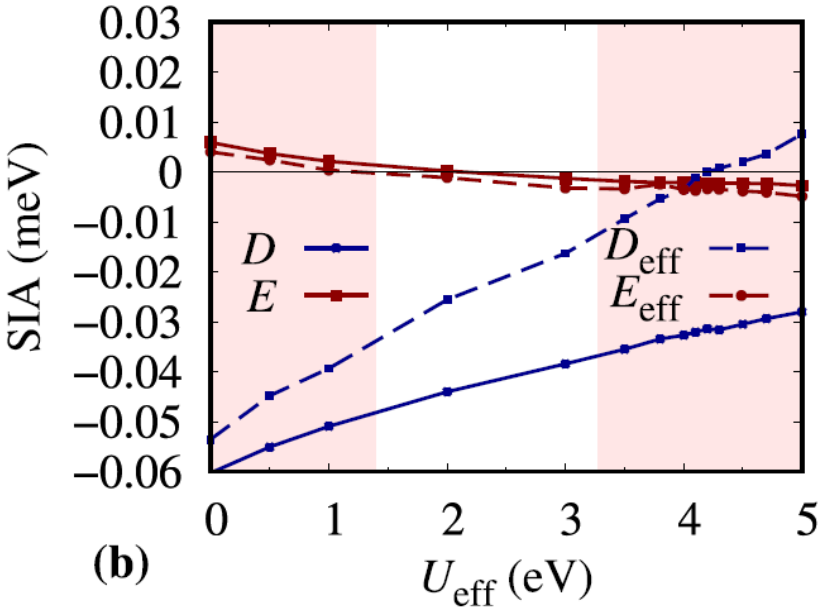

CrSBr: tunability of magnetic properties IV

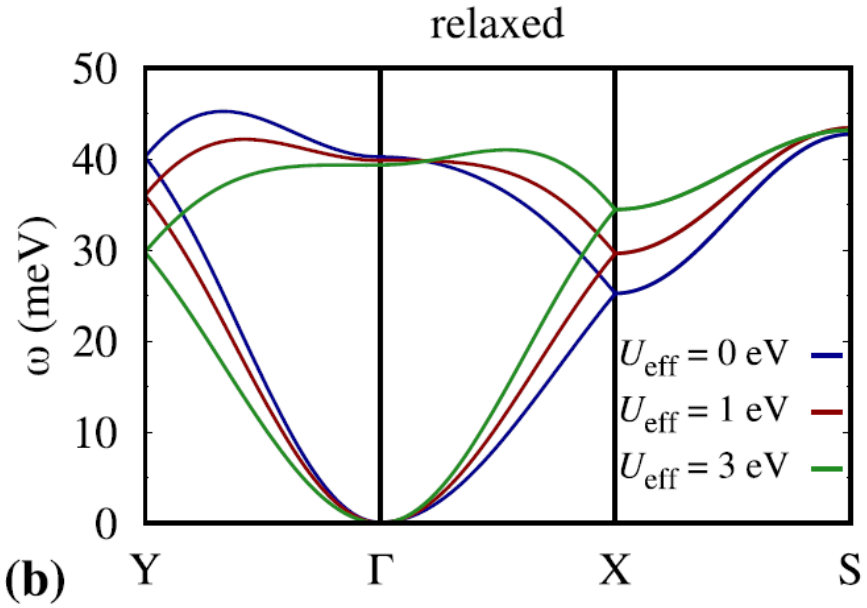

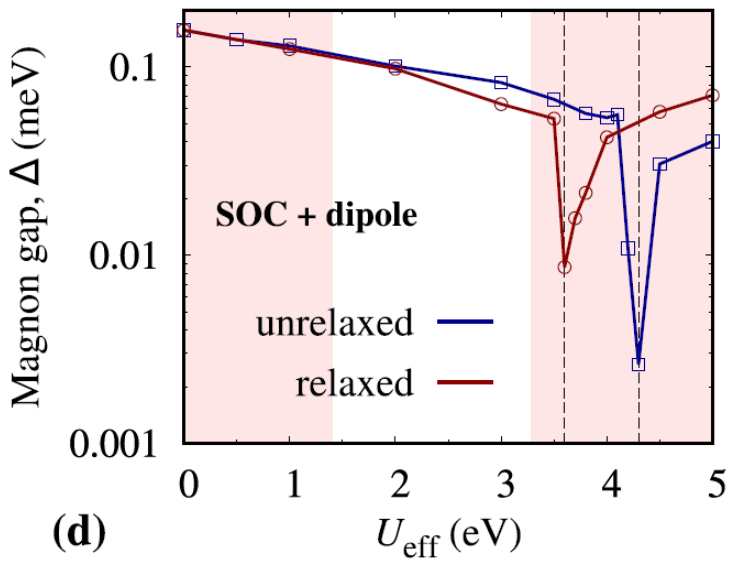

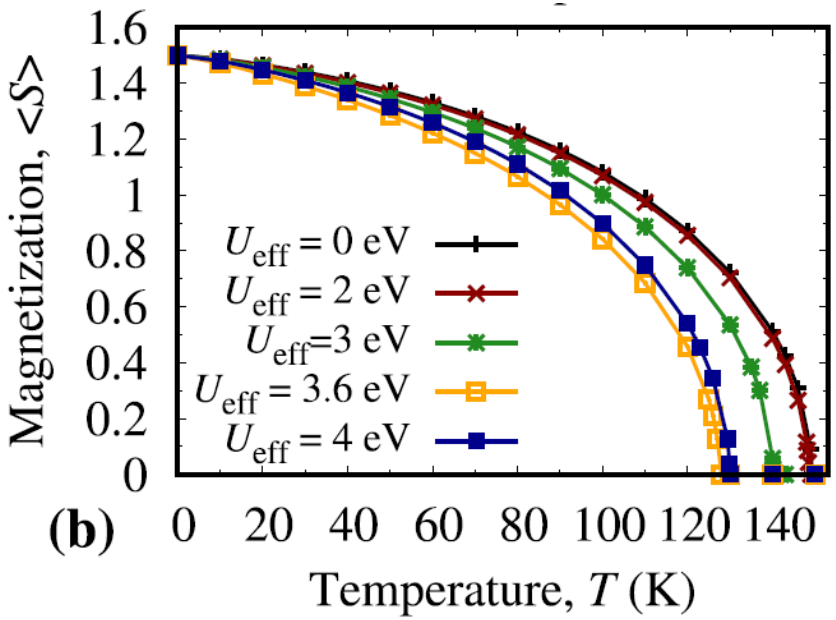

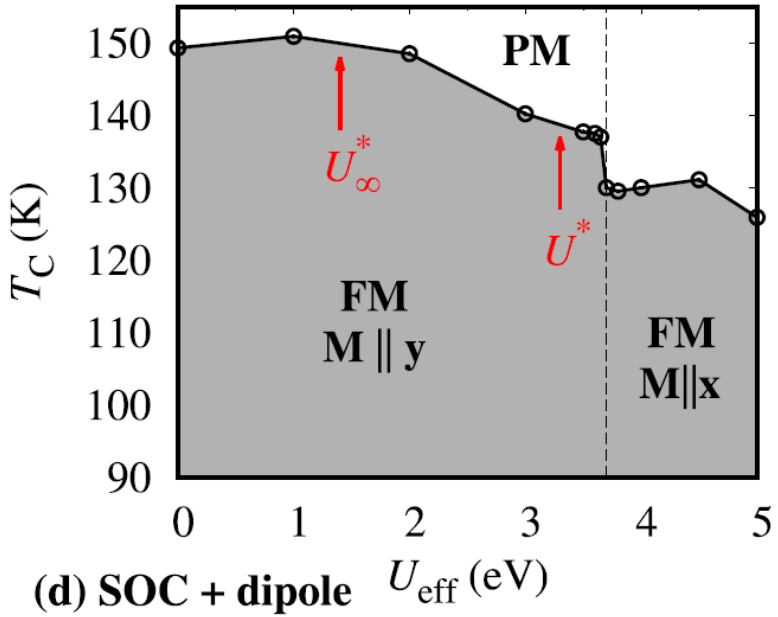

Hyperbolic polaritons in (bulk) CrSBr

Just to remind: crystallooptics

$$\vec{k} = k_0 \vec{n}, \qquad k_0 = \frac{\omega}{c} \qquad \det\left| n^2 \delta_{ij} - n_i n_j - \varepsilon_{ij}(\omega) \right| = 0$$

$$\varepsilon_{ij}(\omega) = \delta_{ij} + \frac{4\pi i}{\omega}\sigma_{ij}(\omega)$$

Main axes $\varepsilon_{ij} = \varepsilon_i \delta_{ij}$

If $\varepsilon_x \varepsilon_y < 0$

$$n_z = 0$$
$$n^2 = \varepsilon_z$$
$$\frac{n_x^2}{\varepsilon_y} + \frac{n_y^2}{\varepsilon_x} = 1$$

$$\frac{k_x^2}{|\varepsilon_y|} = \frac{k_y^2}{|\varepsilon_x|}, \qquad k >> k_0 \qquad (c \to \infty)$$

Anisotropy can result in the formation of additional types of electromagnetic waves!

Hyperbolic polaritons in bulk CrSBr II

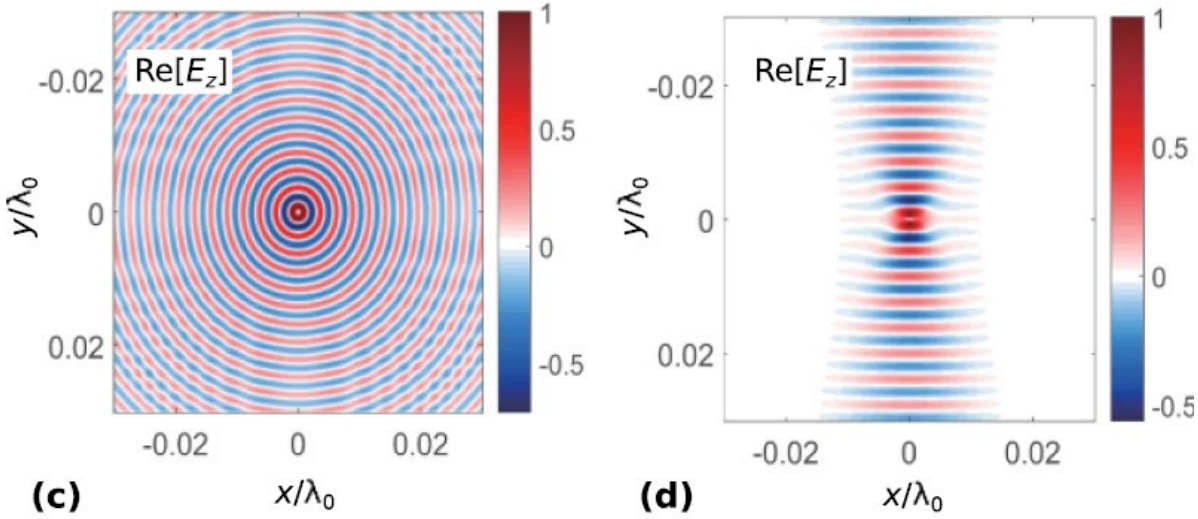

Distribution of electric fields for elliptic and hyperbolic polaritons

Chang P-H, Lin C and Helmy A S 2022 Field canalization using anisotropic 2D plasmonics *npj 2D Mater. Appl.* 6 5

In CrSBr: electronic structure and thus optical properties are sensitive to magnetic order

Paramagnetic electronic structure of CrSBr: Comparison between *ab initio GW* theory and angle-resolved photoemission spectroscopy

Marco Bianchi,[1] Swagata Acharya,[2,3] Florian Dirnberger,[4] Julian Klein,[5] Dimitar Pashov,[6] Kseniia Mosina,[7] Zdenek Sofer,[7] Alexander N. Rudenko,[3] Mikhail I. Katsnelson,[3] Mark van Schilfgaarde,[6,2] Malte Rösner,[3] and Philip Hofmann[1,*]

PHYSICAL REVIEW B **107**, 235107 (2023)

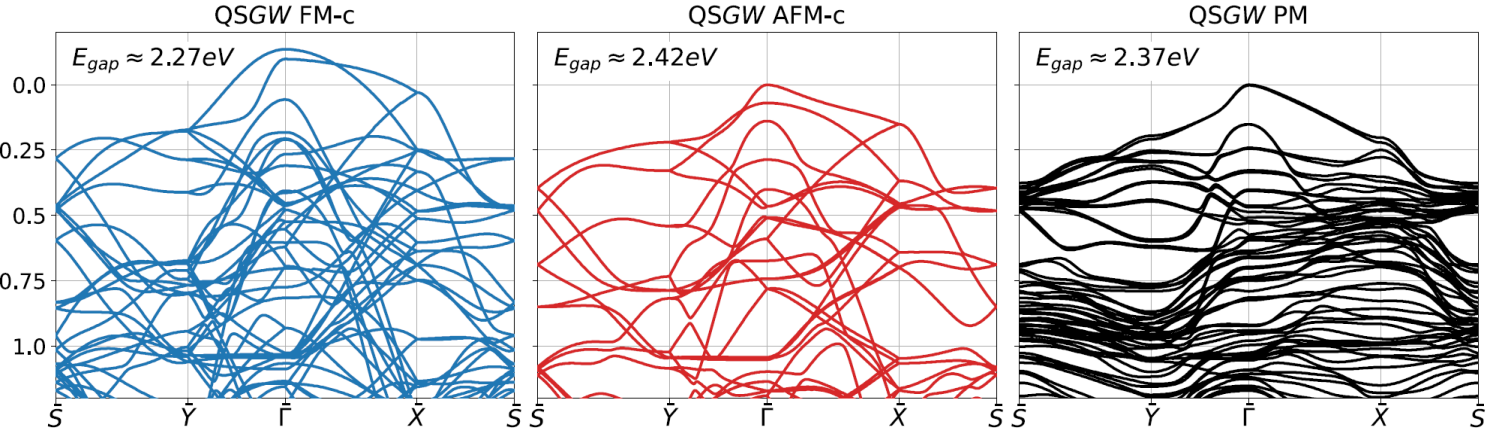

Valence bands in QSGW

Hyperbolic polaritons in bulk CrSBr III

nature communications

Article

https://doi.org/10.1038/s41467-023-44100-6

Hyperbolic exciton polaritons in a van der Waals magnet

Francesco L. Ruta[1,2,12] ✉, Shuai Zhang[1,12] ✉, Yinming Shao[1,12], Samuel L. Moore[1], Swagata Acharya[3], Zhiyuan Sun[1], Siyuan Qiu[1], Johannes Geurs[1,4], Brian S. Y. Kim[1,5], Matthew Fu[1], Daniel G. Chica[6], Dimitar Pashov[7], Xiaodong Xu[8,9], Di Xiao[8,9], Milan Delor[6], X-Y. Zhu[6], Andrew J. Millis[1,10], Xavier Roy[6], James C. Hone[5], Cory R. Dean[1], Mikhail I. Katsnelson[11], Mark van Schilfgaarde[3] & D. N. Basov[1] ✉

Experiment: observation of hyperbolic polariton at low enough temperature

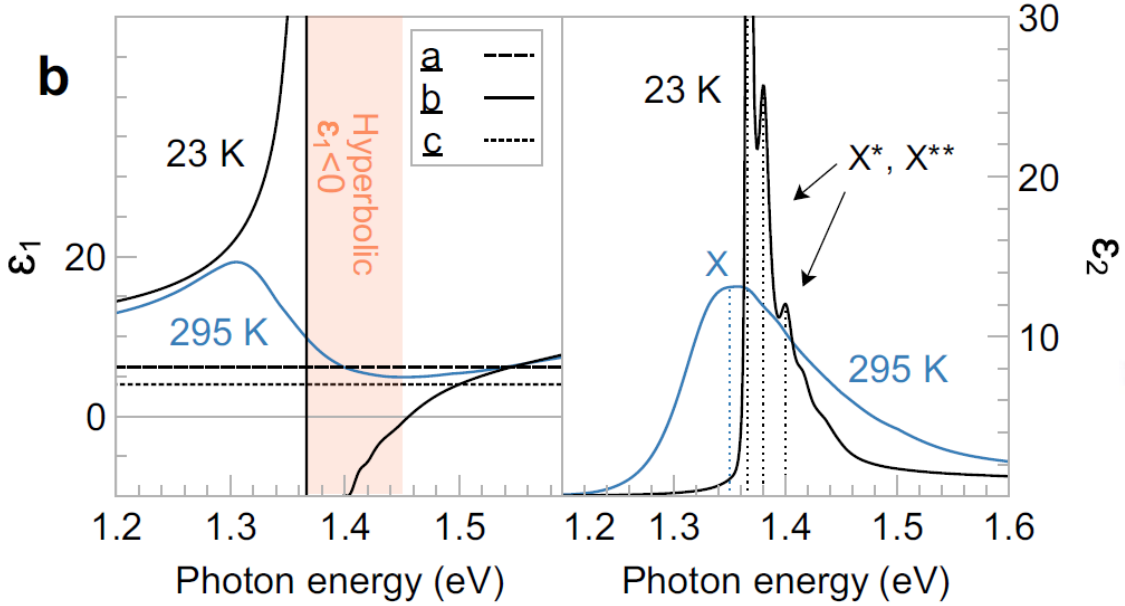

Resonances associated to excitons (confirmed by QSGW+BSE calculations)

AFM order is crucially important!

Hyperbolic polaritons in bulk CrSBr IV

Hyperbolic region from experiment

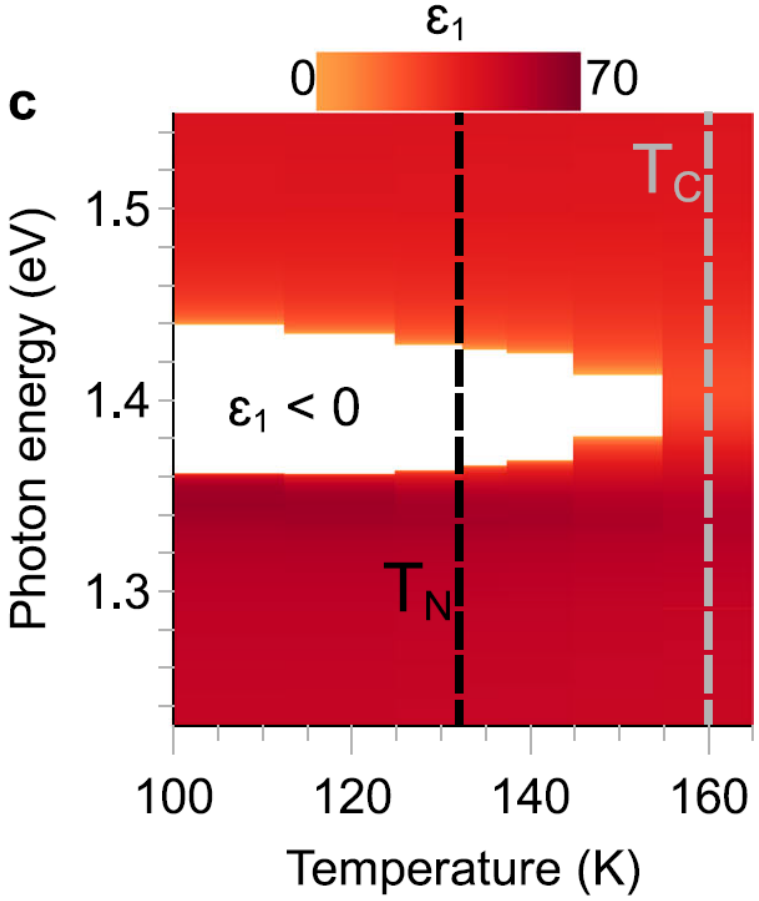

Exciton spectral weight (experiment, cf two QSGW values for AFM and PM states)

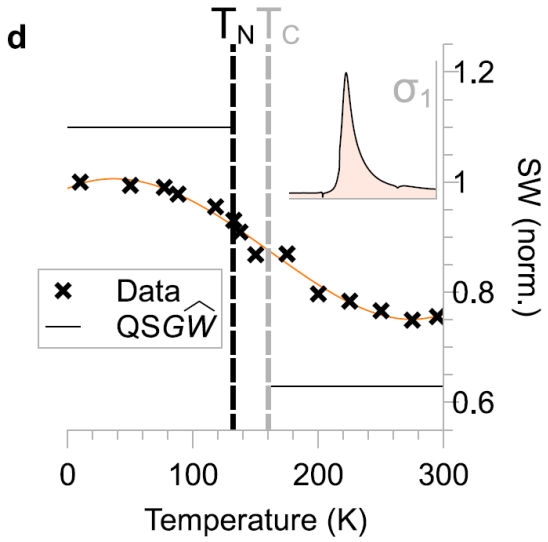

Exciton decomposition (calculations)

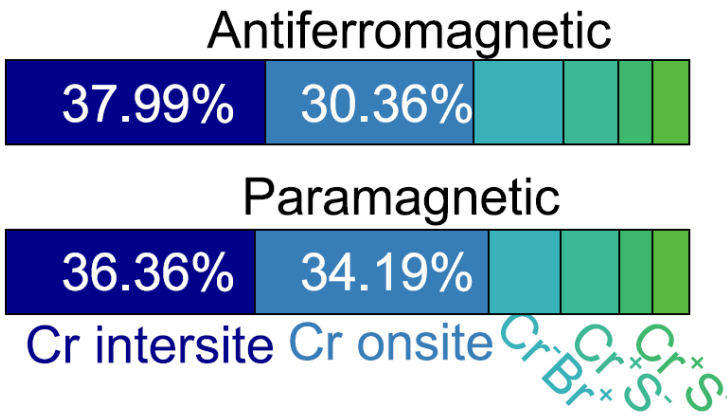

Lattice effects and magnetism in Fe_3GeTe_2

Electron transport and scattering mechanisms in ferromagnetic monolayer Fe_3GeTe_2

npj 2D Materials and Applications (2023)7:52

Danis I. Badrtdinov[1]✉, Georgy V. Pushkarev[2], Mikhail I. Katsnelson[1] and Alexander N. Rudenko[1]✉

Metallic 2D FM with high Curie temperature (above 200 K)

Comparison of magnon and phonon scattering processes

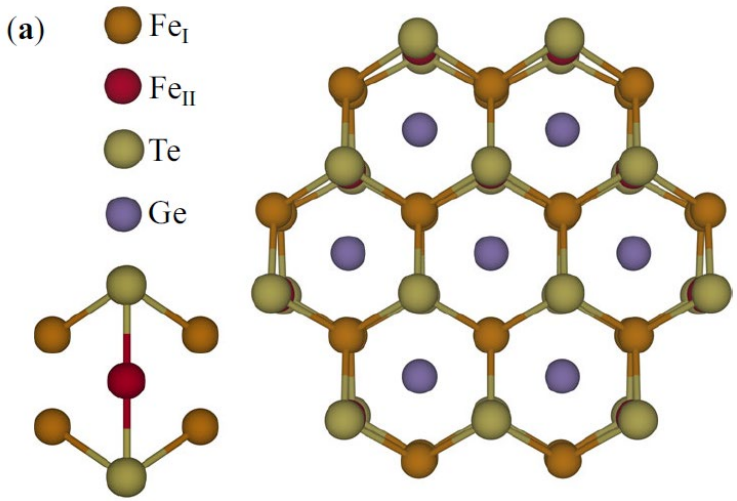

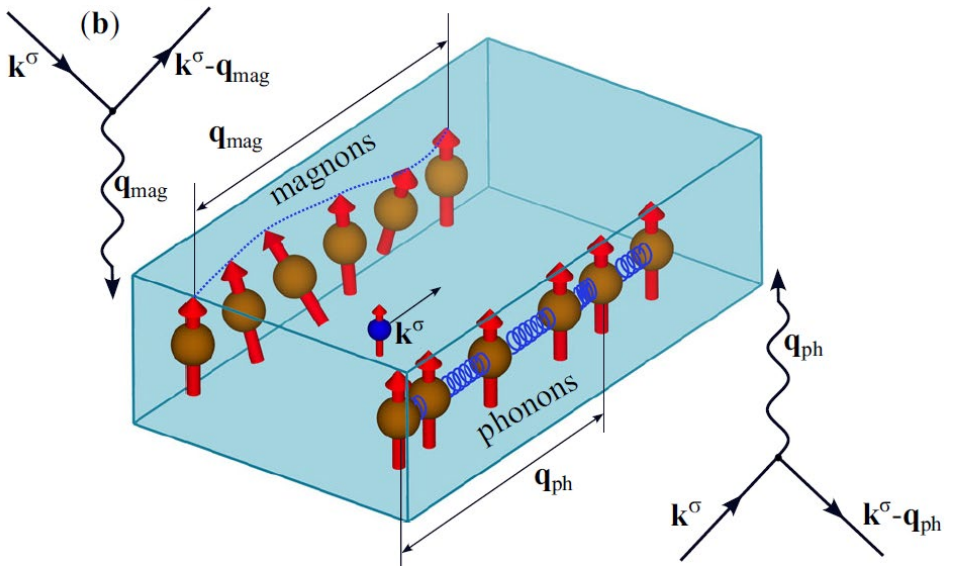

Lattice effects and magnetism in Fe_3GeTe_2 II

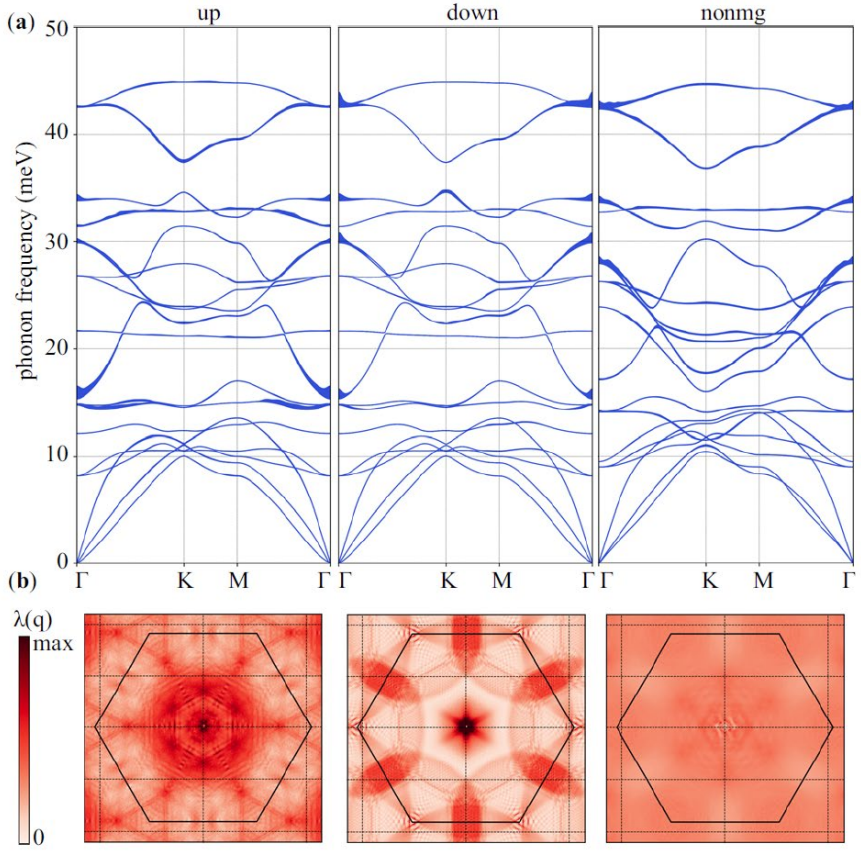

Fig. 3 Phonon dispersion curves and momentum-resolved electron-phonon coupling calculated for the ferromagnetic and nonmagnetic phases of monolayer Fe_3GeTe_2. a Phonon dispersion curves shown with the spin-dependent linewidth that is proportional to $\mathrm{Im}[\Pi^{\sigma}_{\mathbf{q}\nu}] = \pi N_F^{\sigma} \lambda^{\sigma}_{\mathbf{q}\nu} \omega^2_{\mathbf{q}\nu}$. **b** Momentum-resolved electron-phonon coupling constant $\lambda^{\sigma}_{\mathbf{q}} = \sum_{\nu} \lambda^{\sigma}_{\mathbf{q}\nu}$.

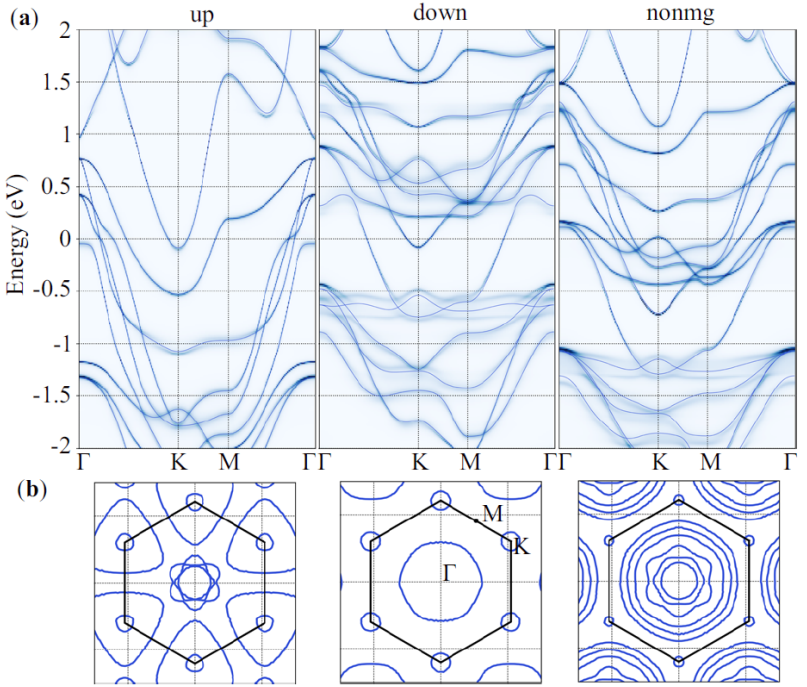

Fig. 2 Spin-dependent electron spectral functions and Fermi contour maps for the ferromagnetic and nonmagnetic phases of monolayer Fe_3GeTe_2. a Spectral functions $A^{\sigma}_{\mathbf{k}}(\omega, T) = -1/\pi\, \mathrm{Im}[G^{\sigma}_{\mathbf{k}}(\omega, T)]$ calculated in the presence of the electron-phonon interactions for $T = 100$ K for the states near the Fermi level. Original DFT band structure is shown by the blue solid line. Zero energy corresponds to the Fermi energy. **b** The corresponding Fermi contour maps.

Lattice effects and magnetism in Fe_3GeTe_2 III

Effective electron-phonon coupling constant by simple interpolation

$$\lambda^{\sigma}(T) = \lambda_{\text{nonmg}} + \left[\lambda^{\sigma} - \lambda_{\text{nonmg}}\right]\frac{\langle S_z\rangle}{S}$$

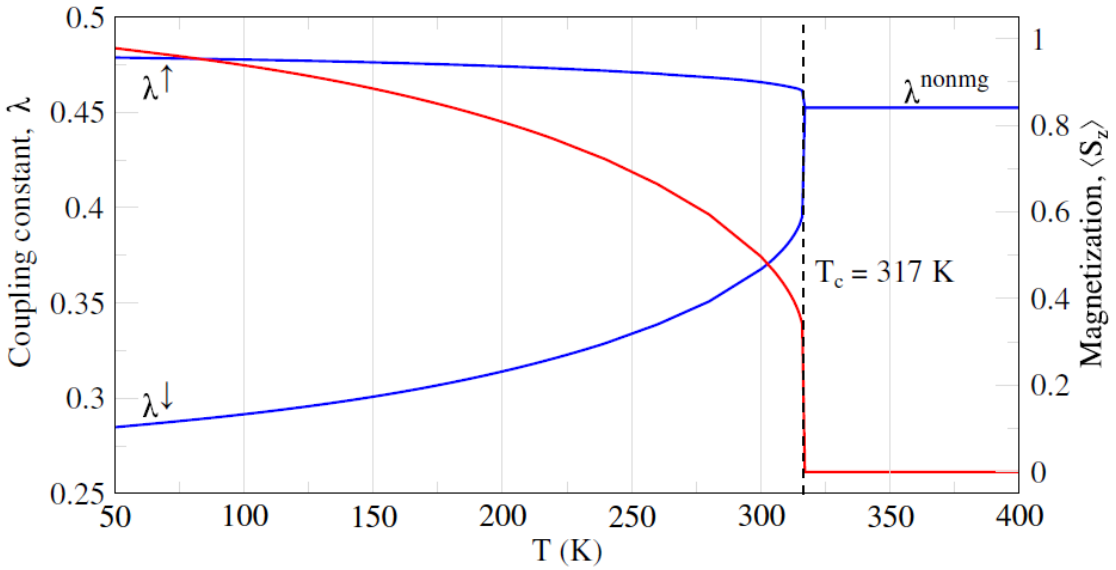

Magnetization from exchange parameters by magnetic force theorem plus generalized Tyablikov approximation

$$J_{ij} = \frac{1}{2\pi S^2}\int_{-\infty}^{E_F} d\varepsilon\, \mathrm{Im}\left[\Delta_i G_{ij}^{\downarrow}(\varepsilon)\Delta_j G_{ji}^{\uparrow}(\varepsilon)\right]$$

$$\hat{\mathcal{H}}_{\mu\nu}^{SW}(\mathbf{q}) = \left[\delta_{\mu\nu}[A + \sum_{\chi} J_{\mu\chi}(\mathbf{0})] - J_{\mu\nu}(\mathbf{q})\right]\langle S_z\rangle$$

$$\langle S_z\rangle = S\frac{1 + 2\sum_{\mathbf{q}\nu} b_{\mathbf{q}\nu}}{1 + 3\sum_{\mathbf{q}\nu} b_{\mathbf{q}\nu} + 3\left(\sum_{\mathbf{q}\nu} b_{\mathbf{q}\nu}\right)^2}$$

$$b_{\mathbf{q}\nu} = \left(\exp[\hbar\omega_{\mathbf{q}\nu}/k_B T] - 1\right)^{-1}$$

Lattice effects and magnetism in Fe_3GeTe_2 IV

Transport properties

$$\sigma_{xx}^{\sigma} = -\frac{e^2}{\Omega}\sum_{n\mathbf{k}} \frac{\partial f_{n\mathbf{k}}^{\sigma}}{\partial \varepsilon_{n\mathbf{k}}^{\sigma}} \tau_{n\mathbf{k}}^{\sigma} \left[v_{n\mathbf{k}\sigma}^{x}\right]^2$$

$$1/\tau_{n\mathbf{k}}^{\sigma} = \frac{2}{\hbar}\mathrm{Im}\Sigma_{n\mathbf{k}}^{\sigma}$$

$$v_{n\mathbf{k}\sigma}^{x} = \partial\varepsilon_{n\mathbf{k}}^{\sigma}/\partial(\hbar k_x)$$

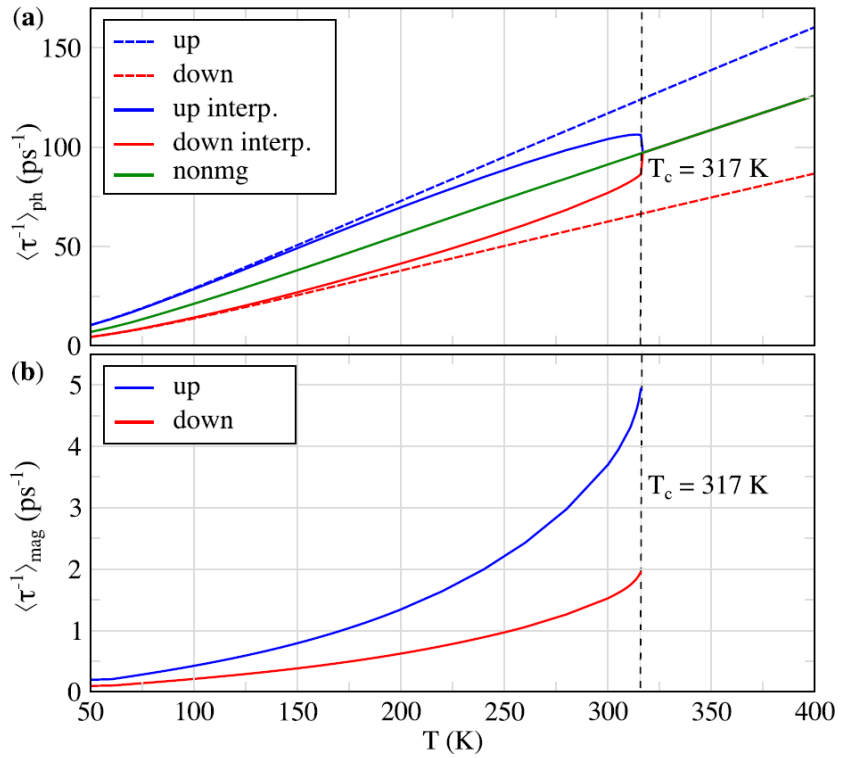

$$\Sigma_{n\mathbf{k}}^{\sigma}(\omega,T) = \sum_{m\,\mathbf{q}\nu} \left|g_{mn,\nu}^{\sigma}(\mathbf{k},\mathbf{q})\right|^2 \times$$

$$\times \left[\frac{b_{\mathbf{q}\nu}+f_{m\mathbf{k}+\mathbf{q}}^{\sigma}}{\omega-\varepsilon_{m\mathbf{k}+\mathbf{q}}^{\sigma}+\hbar\omega_{\mathbf{q}\nu}-i\eta} + \frac{b_{\mathbf{q}\nu}+1-f_{m\mathbf{k}+\mathbf{q}}^{\sigma}}{\omega-\varepsilon_{m\mathbf{k}+\mathbf{q}}^{\sigma}-\hbar\omega_{\mathbf{q}\nu}-i\eta}\right]$$

$$g_{mn,\nu}^{\sigma}(\mathbf{k},\mathbf{q}) = \sqrt{\frac{\hbar}{2m_0\omega_{\mathbf{q}\nu}}}\left\langle\psi_{m\mathbf{k}+\mathbf{q}}^{\sigma}\middle|\partial_{\mathbf{q}\nu}V^{\sigma}\middle|\psi_{n\mathbf{k}}^{\sigma}\right\rangle$$

and similar for magnons

$$\Sigma_{n\mathbf{k}}^{\uparrow}(\omega,T) = 2I^2\langle S_z\rangle\sum_{\mathbf{q}\nu}\frac{b_{\mathbf{q}\nu}+f_{n\mathbf{k}+\mathbf{q}}^{\downarrow}}{\omega-\varepsilon_{n\mathbf{k}+\mathbf{q}}^{\downarrow}+\hbar\omega_{\mathbf{q}\nu}-i\eta}$$

$$\Sigma_{n\mathbf{k}}^{\downarrow}(\omega,T) = 2I^2\langle S_z\rangle\sum_{\mathbf{q}\nu}\frac{b_{\mathbf{q}\nu}+1-f_{n\mathbf{k}-\mathbf{q}}^{\uparrow}}{\omega-\varepsilon_{n\mathbf{k}-\mathbf{q}}^{\uparrow}-\hbar\omega_{\mathbf{q}\nu}-i\eta}.$$

Dependence of phonon contribution on magnetization
Is much more important than direct magnon scattering

$$I = \frac{1}{2SN_F}\sum_{m\,\mathbf{k}\sigma}\left(\varepsilon_{m\mathbf{k}}^{\uparrow}-\varepsilon_{m\mathbf{k}}^{\downarrow}\right)\frac{\partial f_{m\mathbf{k}}^{\sigma}}{\partial\varepsilon_{m\mathbf{k}}^{\sigma}}$$

Lattice effects and magnetism in Fe_3GeTe_2 V

Phonon-induced renormalization of exchange interactions in metallic two-dimensional magnets

Danis I. Badrtdinov, Mikhail I. Katsnelson, and Alexander N. Rudenko*

PHYSICAL REVIEW B **110**, L060409 (2024)

Magnetic force theorem for exchange in correlated systems

$$J_{ij} = 2\mathrm{Tr}_{\omega L}(\Sigma_i^s G_{ij}^{\uparrow} \Sigma_j^s G_{ji}^{\downarrow})$$

MIK & Lichtenstein 2000, for review see our recent review

$$\Sigma_i = \Sigma_i^c + \vec{\Sigma}_i^s \vec{\sigma}$$

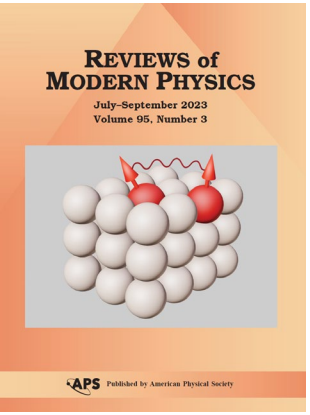

The idea (very simple and straightforward!): include electron-phonon contributions into the self-energy – much simpler than explicitly do calculations for distorted systems

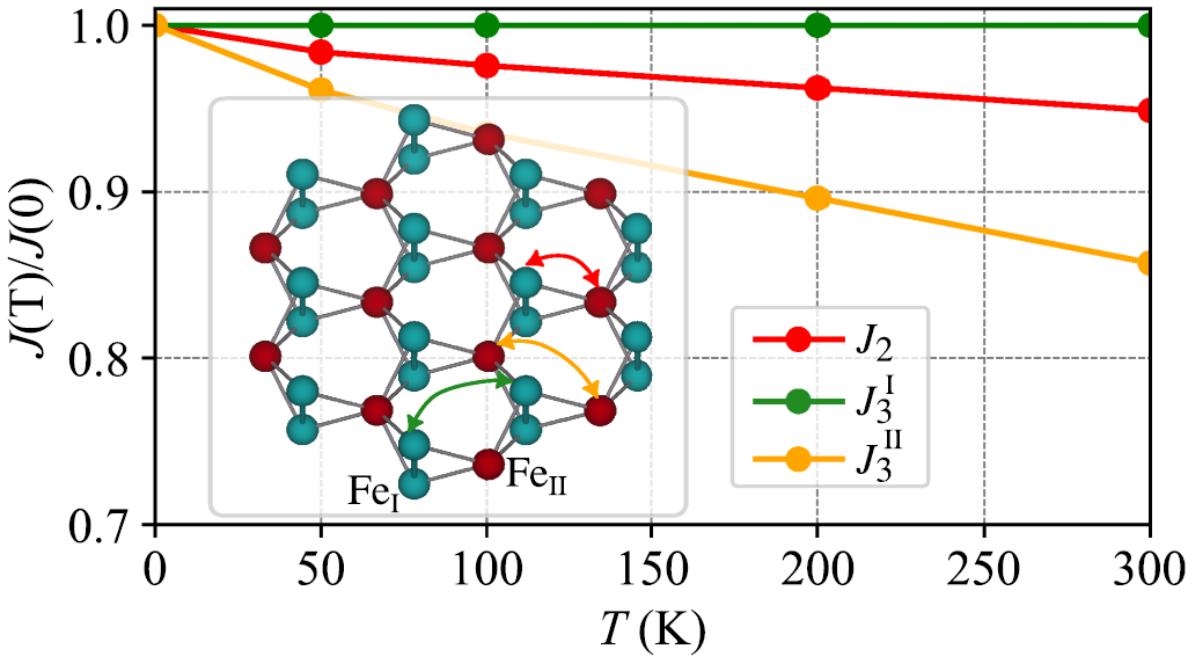

Lattice effects and magnetism in Fe_3GeTe_2 VI

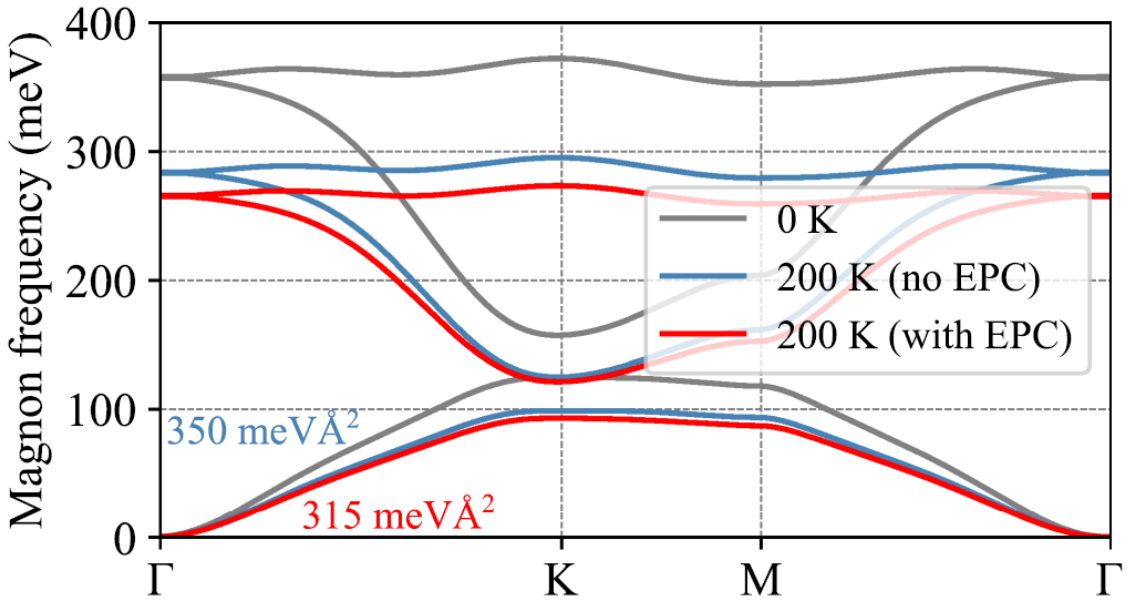

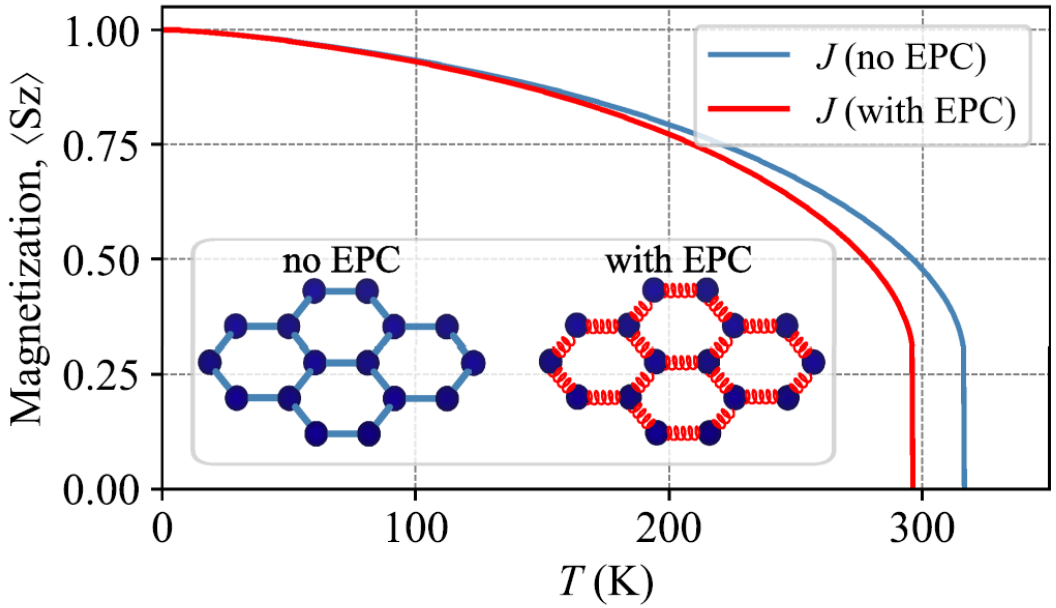

Curie temperature decreased by approx. 10%

Conclusions

- Known 2D magnets are strongly correlated, go beyond DFT (but GW-like methods seem to be sufficient)
- Be careful with dipole-dipole interactions, they are not just shape anisotropy
- Importance of p-d hybridization in CrX_3, different magnetooptical properties for X = Br and X = I
- Opportunity of electron self-trapping
- Tunability of magnetic properties via substrate
- Highly anisotropic CrSBr, very special optics sensitive to magnetism
- Nontrivial interplay of electron-magnon and electron-phonon interactions in 2D metallic magnets, phonons are important!

Many thanks to all collaborators and many thanks to you for your attention